ROTATING AND EXPANDING GAS IN post-AGB NEBULAE

V. Bujarrabal (v.bujarrabal@oan.es),
J. Alcolea, A. Castro-Carrizo, H. van Winckel, M. Santander-García, R. Neri, and R. Lucas

INTRODUCTION

Together with the well-known, usually observed young planetary nebulae (PNe) and protoplanetary nebulae (PPNe), which are very massive and intense in all wavelengths, there is also a group of post-AGB stars surrounded by low mass nebulae that are usually identified from their stellar properties (van Winckel 2003, Alcolea & Bujarrabal 1991, etc). A good deal of these objects, about one half of the total, show a remarkable NIR excess, which is often attributed to the emission of hot dust kept close to the star, perhaps in a stable (i.e. rotating) disk (e.g. van Winckel 2003, van Aarle et al. 2012). These objects show other properties, like the presence of highly processed grains and signs of reaccretion by the central star, that support the existence of long-lived components in the inner nebula. It is also remarkable that the central stars are found to be systematically close binaries (de Ruyter et al. 2005 and references therein). The future evolution of this class of objects is uncertain, since the stellar temperatures are still low, less than about 10000 K, and, as we will see, the total ejected mass remains very moderate.

First rotating disk identified in a young planetary nebula: Previous PdB maps of CO emission in the Red Rectangle

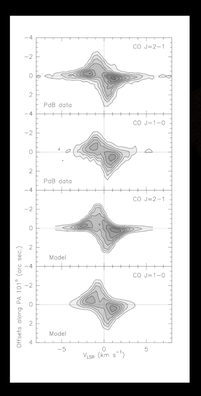

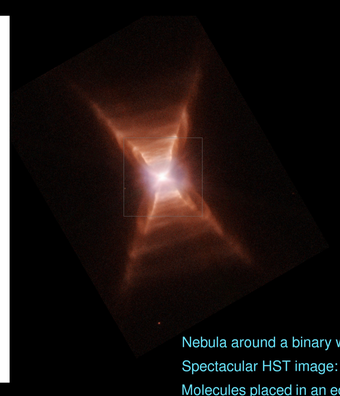

Nebula around a binary with NIR excess
Spectacular HST image: axisymmetric nebula
Molecules placed in an equatorial rotating disk

Detailed analysis of Herschel data of the Red Rectangle: also slow outflow

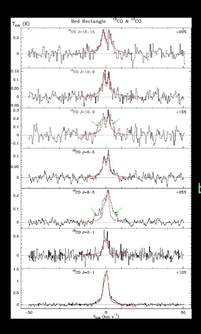

Typical line profiles of disks

fitting by sophisticated 2-D non-local models
=> Low velocities and mass ($\sim 6\ 10^{-3}$ $M_\odot$)

but: arrows: wing excess not explained by disk
=> low-mass outflow ($\sim 10^{-3}$ $M_\odot$)
expanding at low velocity (~ 10 km s^{-1})

Very different from 'standard' PPNe !!

Disk velocity, density, and temperature

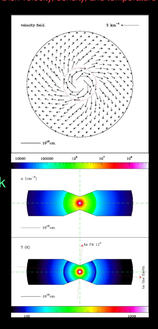

Expanding component derived indirectly, but recently confirmed by ALMA (spectacular) maps!

Disk-like spectra from NIR-excess post-AGB stars

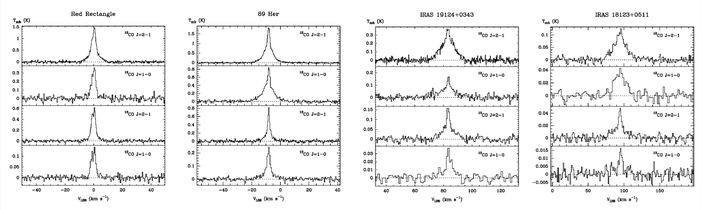

Out of 14 well-observed objects, 11 show narrow profiles indicative of rotating disks
+ 4 more objects detected in the southern hemisphere

Relatively intense wings suggest the presence of also an outflow in at least 8 objects (confirmed in the 3 objects mapped up to date)

other examples :

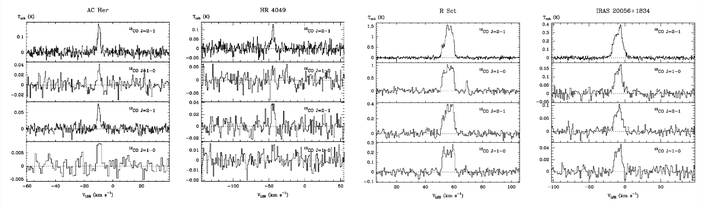

Often weak emission, much weaker than in 'standard' PPNe

In 2 cases (R Sct and IRAS 20056+1834) the expanding component seems dominant

Post-AGB stars with NIR excess: CO 30m observations

Source	observed coordinates J2000		$F_{25\mu}$ Jy	$F_{60\mu}$ Jy	luminosity $L_\odot$	distance pc	sp. type	V_*(LSR) km s^{-1}	comments
RV Tau	04:47:06.73	+26:10:45.6	18.1	6.5	3500	2200[1]	G2-M2	+17	RV Tau variable
DY Ori	06:06:14.91	+13:54:19.1	14.9	4.2	1600	2000[1]	G0 I	–16	RV Tau variable
Red Rectangle	06:19:58.22	–10:38:14.7	456.1	173.1	6000	710[2]	B9	0	interferometric CO maps
U Mon	07:30:47.47	–09:46:36.8	88.4	26.6	4000	800[1]	F8-K0 I	+9	RV Tau variable
AI CMi	07:35:41.15	+00:14:58.0	68.1	18.5	3000[3]	1500[3]	G5 I	+33	
HR 4049	10:18:07.59	–28:59:31.2	9.6	1.8	2900	650[4]	A6 I	–45	well studied inner disk
89 Her	17:55:25.19	+26:03:00.0	54.5	13.4	9200	1000[5]	F2 I	–8	interferometric CO maps
IRAS 18123+0511	18:14:49.39	+05:12:55.7	11.0	4.2	3000[3]	3500[3]	F2	+99	
AC Her	18:30:16.24	+21:52:00.6	65.3	21.4	3500	1100[1]	F2-K4 I	–10	previous tent. det., RV Tau variable
R Sct	18:47:28.95	–05:42:18.5	9.3	8.2	14000	1000[5]	G0-K0 I	+55	previous det., pec. RV Tau variable
IRAS 19125+0343	19:15:01.18	+03:48:42.7	26.5	7.8	3000[3]	1500[3]	F2	+84	
IRAS 19157–0247	19:18:22.71	–02:42:10.9	7.2	2.5	3000[3]	2900[3]	F3	+49	
IRAS 20056+1834	20:07:54.62	+18:42:54.5	18.0	5.4	3000[3]	3000[3]	G0	~0	edge-on disk
R Sge	20:14:03.75	+16:43:35.1	7.5	2.1	2500	2500[1]	G0-K0 I	+28	RV Tau variable

Distance estimate: [1]: P-L relation for RV Tau variables. [2]: Men'shchikov et al. (2002). [3]: Assumed luminosity. [4]: Corrected parallax (Acke et al. 2013). [5]: Hipparcos parallax.

HIGH DETECTION RATE: 11 out of 14 sources
and systematically show disk-like profiles !! (similar to the RedRect)

Post-AGB stars with NIR excess: CO observations of southern sources

Source	observed coordinates J2000		$F_{25\mu}$ Jy	$F_{60\mu}$ Jy	luminosity $L_\odot$	distance pc	sp. type	V_*(LSR) km s^{-1}	comments
AR Pup	08:03:01.65	–36:35:47.9	94.3	26.1	3500	2800[1]	F0I	+29	RV Tau variable
IRAS 08544–4431	08:56:14.18	–44:43:10.7	158.8	56.3	3000[2]	550[2]	F3	+45	previous det., pec. RV Tau variable
IW Car	09:26:53.30	–63:37:48.9	96.2	34.5	3000	1000[1]	A4I	–25	RV Tau variable
IRAS 10174–5704	10:19:16.89	–57:19:26.0	60.3	16.1	3000[2]	850[2]	G8I	+3	
IRAS 10456–5712	10:47:38.40	–57:28:02.7	115.5	30.9	3000[2]	600[2]	M1	–9	
HD 95767	11:02:04.31	–62:09:42.8	15.7	10.9	3000[2]	1400[2]	F3II	–32	
RU Cen	12:09:23.81	–45:25:34.8	11.0	5.7	2500	2200[1]	G2	–35	RV Tau variable
HD 108015	12:24:53.50	–47:09:07.5	33.23	8.0	3000[2]	1800[2]	F4I	–2	
IRAS 15469–5311	15:50:43.80	–53:20:43.3	42.1	15.5	3000[2]	1200[2]	F3	–14	
IRAS 15556–5444	15:59:32.57	–54:53:20.4	17.8	7.1	3000[2]	1700[2]	F8	?	

Distance estimate: [1]: P-L relation for RV tau stars. [2]: assumed luminosity.

5 sources show strong galactic contamination => less meaningful statistics
nevertheless several detections

Mass of rotating disks and total nebulae

Source	mass $M_\odot$	typical size "	typical size cm	comments
RV Tau	$< 8\ 10^{-3}$	<0.5	$<1.3\ 10^{16}$	
DY Ori	$2\ 10^{-3}$	0.37	$1.1\ 10^{16}$	
Red Rectangle	$6.6\ 10^{-3}$			total neb.
Red Rectangle	$6\ 10^{-3}$	2	$2.3\ 10^{16}$	disk
U Mon	$< 9\ 10^{-4}$	<0.4	$< 5\ 10^{15}$	
AI CMi	$1.9\ 10^{-2}$	1.2	$2.7\ 10^{16}$	prob. exp. comp.
HR 4049	$6.3\ 10^{-4}$	0.6	$6\ 10^{15}$	
89 Her	$2.7\ 10^{-2}$			total neb.
89 Her	$1.4\ 10^{-2}$	1.5	$2.3\ 10^{16}$	disk
IRAS 18123+0511	$4.7\ 10^{-2}$	0.6	$3\ 10^{16}$	prob. exp. comp.
AC Her	$8.4\ 10^{-4}$	0.7	$1.1\ 10^{16}$	
R Sct	$5\ 10^{-2}$			total neb. (complex prof.)
R Sct	$\sim 6.9\ 10^{-3}$	~1	$\sim 1.5\ 10^{16}$	disk
IRAS 19125+0343	$1.3\ 10^{-2}$	1	$2.3\ 10^{16}$	prob. exp. comp.
IRAS 19157–0247	$1.4\ 10^{-2}$	0.7	$3\ 10^{16}$	
IRAS 20056+1834	10^{-1}			total neb. (complex prof.)
IRAS 20056+1834	$\sim 2.5\ 10^{-2}$	~0.6	$\sim 1.7\ 10^{16}$	disk
R Sge	$< 9\ 10^{-3}$	<0.3	$<7\ 10^{15}$	
IRAS 08544–4431	$\sim 7.7\ 10^{-3}$	2.2	$1.8\ 10^{16}$	from ^{12}CO data
IW Car	$\sim 5.3\ 10^{-3}$	1.3	$2\ 10^{16}$	from ^{12}CO data
HD 95767	$\sim 1.2\ 10^{-3}$	0.6	$1.3\ 10^{16}$	from ^{12}CO data
HD 108015	$\sim 2.3\ 10^{-2}$	1.2	$3\ 10^{16}$	from ^{12}CO data

From optically thin line ^{13}CO J=1–0

Low-mass values: $\sim 10^{-3}$ – 10^{-2} $M_\odot$
(dominant component in most cases)
always < 0.1 $M_\odot$, even including outflows

Mass and velocity of slow outflows

Source	mass $M_\odot$	Velocity km s^{-1}	comments
Red Rectangle	10^{-3}	3 – 13	from low-res. data modelling and recent ALMA maps
AI CMi	$\sim 10^{-2}$	~ 4	from single-dish data, difficult estimate
89 Her	10^{-2}	3 – 7	from PdB maps
R Sct	$\sim 4\ 10^{-2}$	~ 10	from single-dish data, complex profiles
IRAS 20056+1834	$\sim 7\ 10^{-2}$	~ 10	from single-dish data, complex profiles
IRAS 18123+0511	$\sim 10^{-2}$	~ 15	from single-dish data, difficult estimate
IRAS 19125+0343	$4\ 10^{-3}$	5 – 12	unpublished PdB maps
IRAS 08544–4431	$\sim 2\ 10^{-3}$	~ 5	from single-dish data, difficult estimate

Present in at least 8 objects. Relatively good estimates in 3 mapped nebulae
SIGNIFICANT CONTRIBUTION, DOMINANT IN A FEW CASES
–> outflows are probably present in most disk-like nebulae (appear in all those mapped!)

RESULTS

We have observed CO mm-wave emission in 24 objects of this class, using the 30m IRAM telescope and the APEX telescope (Bujarrabal et al. 2013a). CO emission is detected in most observed objects, and the CO lines systematically show the characteristic profiles of rotating disks (narrow, with one or two peaks and low-velocity wings), showing that emission very probably comes from extended disks in rotation. The formation of this kind of profiles in rotating disks is well established from theoretical studies and many observations of disks around young objects (see Bujarrabal & Alcolea 2013, Bujarrabal et al. 2013a, and references therein). The Keplerian or quasi-Keplerian dynamics has been demonstrated by accurate maps of one of our objects, the Red Rectangle, whose molecular component is dominated by an equatorial disk in rotation (Bujarrabal et al. 2005, 2013b). Maps of a second nebula, 89 Her, also show indications of rotation (Bujarrabal et al. 2007). We conclude that rotating disks are present in practically all low-mass post-AGB nebulae showing NIR excess.

In the three objects that have been mapped, the Red Rectangle, 89 Her, and IRAS 19125+0343 (unpublished PdB data), gas in bipolar expansion at low velocity is also found. This expanding component contributes significantly to the CO profile wings (see also discussion on Herschel observation of high-J CO lines by Bujarrabal & Alcolea 2013). Five other objects in our sample show conspicuous line wings, strongly suggesting that in them outflows are also present. Very probably, rotating and expanding gas systematically coexist in these nebulae. From our data, we derive values of the main physical parameters of the disk and, when both components can be discriminated, of the outflows (Bujarrabal et al. 2013a). The total values of the mass are low, usually between 10^{-3} and 10^{-2} M_o, always smaller than 0.1 M_o, significantly smaller than those the 'standard' PPNe and PNe.

The disk is often dominant, except for two objects that show relatively wide profiles. Comparing CO data with data at other wavelengths of the best studied objects of our sample, we find that the molecule-rich component contains practically all the nebular material, being the contributions of PDRs or ionized regions negligible. Therefore, the CO-rich disk contains most of the nebular mass in most of our objects. The derived extent (diameters) of the nebulae are also moderate, of a few 10^{16} cm. The rotation velocities, of about 1-2 km/s, correspond to Keplerian rotation around a central mass of about 1 M_o. Finally, the velocities of the outflows are also quite low, typically between 5 and 10 km/s.

Recent ALMA maps of the Red Rectangle accurately show the structure and dynamics of the nebula (Bujarrabal et al. 2013b). Together with the equatorial disk (which was known from previous PdB data), a bipolar slow flow is also well described. The bipolar outflow is found to occupy the region between the disk and the X-shaped HST image (which would correspond to the inner illuminated boundary of the outflow). We suggest that the expanding gas results from entrainment of disk material by interaction with the fast axial jet that is known to be present in this source.

SUMMARY

We conclude that there is wide class of low-mass post-AGB nebulae characterized by the presence of extended Keplerian disks, which are in most studied cases the dominant nebular component. Many of these objects, probably most of them, present also bipolar outflows with moderate velocities, between 5 and 10 km/s. The mass of the nebulae is always low, typically between 10^{-3} and 10^{-2} M_o.

In one of these objects, the Red Rectangle, CO line maps have accurately shown the structure and dynamics of the nebula. The Red Rectangle is composed of an equatorial rotating disk plus a bipolar outflow that seems to be composed of material extracted from the disk, probably by interaction with axial fast jets. In the other two objects that have been mapped, 89 Her and IRAS 19125+0343, the data suggest similar structures.

High-quality ALMA maps of the Red Rectangle: ^{12}CO and ^{13}CO J=3–2 (0.8 mm)

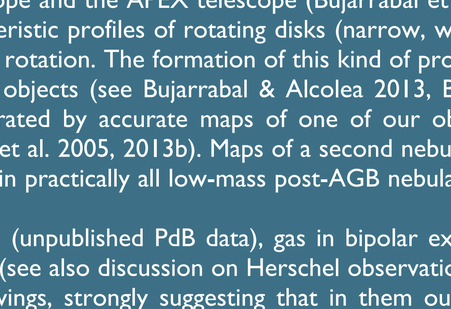

both rotation and expansion !

rotational equatorial disk +

expanding gas between equator and X-shaped nebula

High resolution and sensitivity (see beam in the insets)

outflow almost not det. in ^{13}CO

High-quality ALMA maps of the Red Rectangle: preliminary modeling of ^{12}CO J=3–2

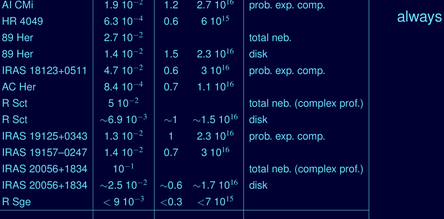

satisfactory simple modeling

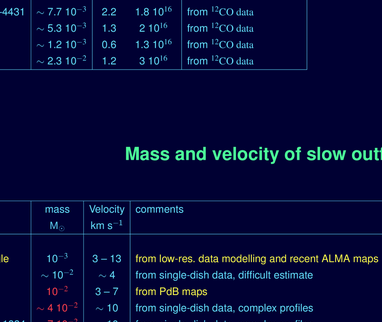

structure, density, and velocity
$T_k \sim 200$ K; rotation not displayed

High-quality ALMA maps of the Red Rectangle: ^{12}CO J=6–5 (0.4 mm)

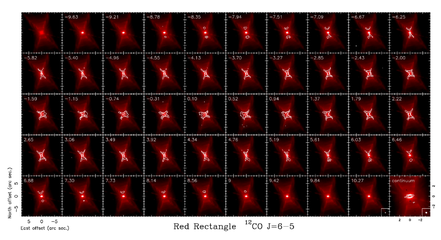

0".25 arcsec resolution !

high exc. line ($\gtrsim$ 100 K)
–> good estimate of T_k

Moderate mass, velocity, and momentum
We interpret: material from the disk entrained by interaction with the axial fast jets
=> short disk lifetime, 1000 - 3000 years (also for 89 Her and IRAS 19125)
We interpret: these results basically apply to all sources of this kind

excellent maps, high resolution, S/N of several hundreds

REFERENCES

This poster is based in recently published results by our group:

Bujarrabal, V., & Alcolea, J. 2013, A&A, 552, A116
Bujarrabal, V., Alcolea, J., Van Winckel, H., Santander-Garcia, M., & Castro-Carrizo, A. 2013a, A&A, 557, A104
Bujarrabal, V., Castro-Carrizo, A., Alcolea, J., et al. 2013b, A&A, 557, L11

Other references:

Acke, B., Degroote, P., Lombaert, R., et al. 2013, A&A, 551, A76
Alcolea, J., & Bujarrabal, V. 1991, A&A, 245, 499
Bujarrabal, V., Castro-Carrizo, A., Alcolea, J., & Neri, R. 2005, A&A, 441, 1031
Bujarrabal, V., van Winckel, H., Neri, R., et al. 2007, A&A, 468, L45
de Ruyter, S., van Winckel, H., Dominik, C., Waters, L.B.F.M., & Dejonghe, H. 2005, A&A, 435, 161
Men'shchikov, A.B., Schertl, D., Tuthill, P. G., Weigelt, G., & Yungelson, L.R. 2002, A&A, 393, 867
van Aarle, E., van Winckel, H., Lloyd Evans, T., et al. 2011, A&A, 530, A90
van Winckel, H. 2003, ARevAA, 41, 391